

Analytical Solution for One-Dimensional Finite Heat Conduction Problem with Heat Balance Integral Method

Braga, Walber F.* and Mantelli, Marcia B. H.†

Heat Pipe Laboratory - Federal University of Santa Catarina, Florianópolis, SC, Brazil

This paper presents an analytical solution for the heat conduction problem within a finite length plate material, considering a prescribed heat flux or prescribed temperature condition at one side of the plate and a prescribed heat flux or prescribed temperature boundary at the opposite side, using the heat balance integral method with an n -temperature profile. The temperature solution obtained by this method is compared with the classical literature solutions.

I. Introduction

CONDUCTION heat transfer is a very important phenomenon to engineering science. Since Fourier's work "La Théorie Analytique de la Chaleur", many mathematics methods has been developed to help understand and to predict the thermal behavior of different materials. Nowadays, the heat conduction is still an interesting phenomenon, presenting several challenging problems such as ablation or phase change, temperature dependent thermal properties, time-variable boundary conditions as well as general coordinate approaches.

The authors of the present paper along the years have been studying analytically the one-dimensional heat conduction and ablations problems using electrical analogy (Braga et al. 2002)¹ and the Heat Balance Integral Method (HBIM). Braga et al. (2003)² presented the semi-infinite conduction problem using the HBIM, subjected to prescribed time-variable heat flux boundary condition on its free surface. These same authors (Braga et al. 2004)³ revisited this same problem, subjected to the free surface time-constant heat flux boundary condition in a finite solid with an insulated opposite surface. In both papers, the pre-ablation and ablation phases were considered. From these previous works, it was observed the need to better understand of the effect of the selected temperature profiles used at the HBIM on the accuracy of the obtained solution.

The HBIM, as presented by Goodman (1964)⁴, is used to obtain an approximate analytical solution. The Goodman's method is based on the Karman-Pohlhausen method and, as expressed by Goodman (1983)⁵, "... although approximate, [the method] provides accuracy adequate for engineering purpose and has the distinct advantage of reducing the problem from one requiring the solution of a partial differential equation, which is relative difficult, to one requiring the solution of an ordinary differential equation, which is relatively easy." The accuracy of the HBIM solution is directly related to the choice of a basic temperature profile that is used. Historically, the polynomial approximations are the most chosen profiles but, as observed by Goodman (1964)⁴, "... there is no a priori guarantee that increasing the order of the polynomial will improve the accuracy".

At the present paper an n -profile is used at the HBIM as the temperature distribution inside a heated finite solid subjected to various boundaries conditions combinations which are presented at Table 1. In this table the left column represents the boundary conditions applied on the right side of the solid (B surface), which can be considered semi-finite (SF) or finite. For the finite case, the following boundary conditions can be considered: prescribed temperature (PT), prescribed heat flux (PH) or convection (C). The first line indicates the boundaries conditions of left side of the body (A surface), which can be the same of the right side plus ablation (A). Some of these boundary condition combinations were already presented at previous works (Braga et al. (2003)², Braga et al. (2004)³ and Braga et al. (2005)⁶⁻⁷) and will not be discussed here. The present paper solves the X marked combinations whose solutions are compared with classical ones.

* Ph.D. Student and Researcher, Mechanical Engineering Department, walber@labtucal.ufsc.br, Member AIAA.

† Professor, Mechanical Engineering Department, marcia@labtucal.ufsc.br, Fellow Member AIAA.

Table 1. Boundary condition combinations.

		A surface			
		PH	PT	C	A
B surface	SF	2005 ⁶	2005 ⁶	2005 ⁷	2003 ²
	PH	X	X		2004 ^{3‡}
	PT	X	X		
	C				

II. General Physical Modeling

The case of a one dimensional finite solid body made of an isotropic material with constant properties is considered. The body is assumed to be at a constant initial temperature (T_0) until the start up of the heating process on the A surface. This heating can occur due a prescribed heat flux (q''_{PA}), a prescribed temperature (T_{PA}) or a convection condition at the mentioned surface. When the prescribed heat flux condition occurs the A surface, the temperature (T_{SA}) can be calculated. Similarly, prescribing the temperature condition, the A surface heat flux (q''_{SA}) can be obtained. The heat is conducted inside the material, developing two different sections: the heated region, which the temperature is affected by the surface imposed heat and the cold region where the material has not felt the presence of the surface heating, remaining at the initial temperature. The position of the interface between those two regions is Δ_B and its distance from the A surface position (Δ_A) is U which is called the heat penetration depth. When the interface position reaches the end of the material i.e, $\Delta_B = L$, the boundary condition of the B surface must be considered and its temperature starts to change. There are, for the B surface, four possible boundaries: semi-finite solid, prescribed heat flux (q''_{PB}), prescribed temperature (T_{PB}) and convection and two variables: the B surface temperature (T_{SB}) and the B surface heat flux (q''_{SB}), can be obtained, similar as A surface. Figure 1 presents the physical modeling scheme of the boundaries combinations that are considered at the present work and those from past papers that are physically important to the present development.

III. Mathematical Modeling

In this section, the mathematical models used to predict the thermal behavior of the above mentioned heat transfer problems are developed.

A heat balance over the body leads to the following well known transient differential heat equation (Eq. (1)).

$$\rho c_p \frac{\partial T}{\partial t} = \frac{\partial}{\partial X} \left(k \frac{\partial T}{\partial X} \right) \quad (1)$$

Using the following variables:

$$\alpha = \frac{k}{\rho c_p} \quad (a)$$

$$\eta = \frac{X}{L} \quad (b)$$

$$\tau = \frac{\alpha t}{L^2} \quad (c)$$

$$\theta = \frac{T - T_0}{T_R - T_0} \quad (d)$$

where α is the heat diffusivity, k is the heat conductivity, ρ is the density, c_p is the heat capacity, L is an arbitrary reference length (usually the length of the solid body), τ is the dimensionless Fourier time, η is the dimensionless space variable, T_R is an arbitrary reference temperature and θ is the dimensionless temperature; and after some algebraic manipulation, one gets the following dimensionless equation, which is the non-dimensional form of Eq. (1):

[‡] The paper presents a time-constant heat flux boundary condition in a finite solid with an insulated opposite surface.

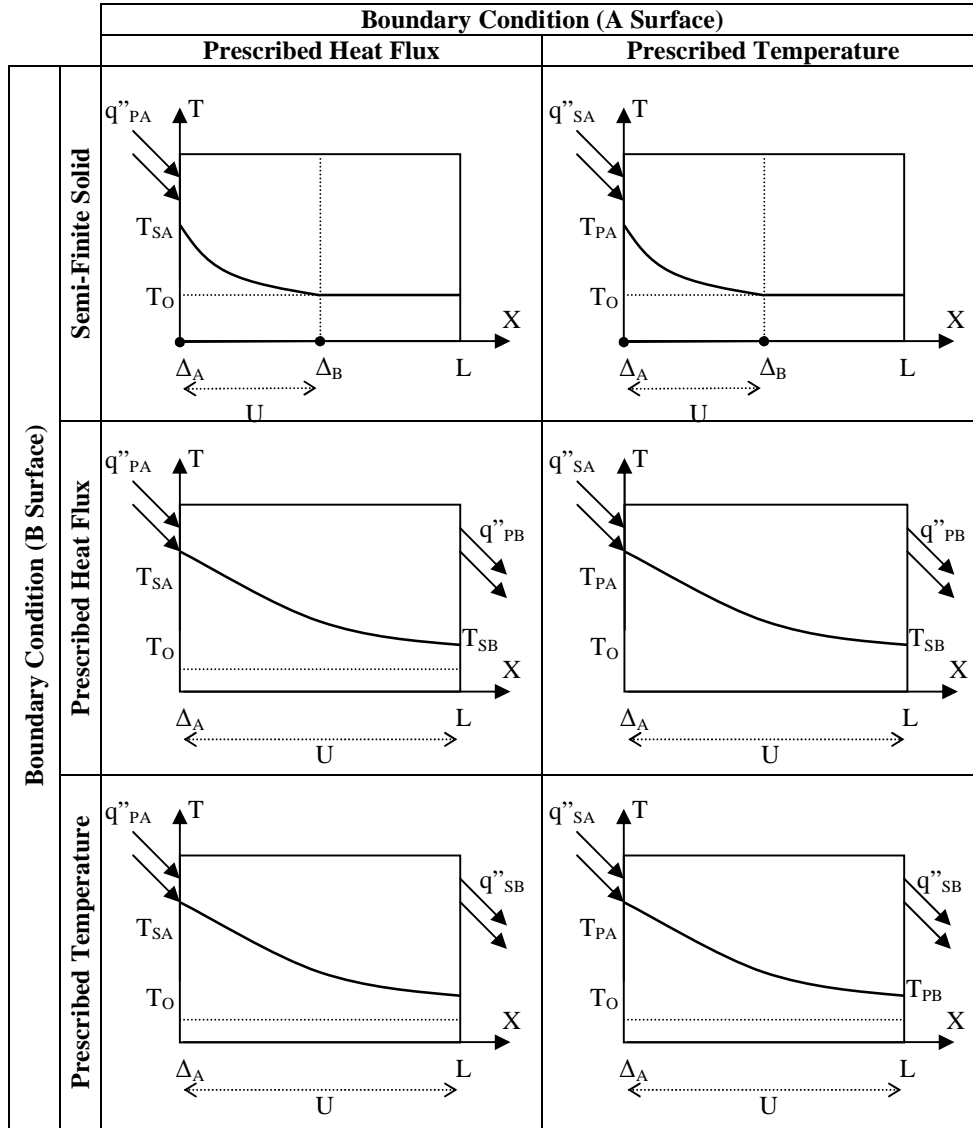


Figure 1. Physical modeling scheme.

$$\frac{\partial \theta}{\partial \tau} = \frac{\partial^2 \theta}{\partial \eta^2}. \quad (3)$$

Based on the Heat Balance Integral Method (HBIM), Eq. (3) is integrated between two points, defined as δ_A and δ_B . The point δ_A is the non-dimensional equivalent of the point Δ_A as the δ_B represents Δ_B . Using the Leibniz rules, it is obtained:

$$\frac{d}{d\tau} \left(\int_{\delta_A}^{\delta_B} \theta d\eta \right) - \theta_B \frac{d\delta_B}{d\tau} + \theta_A \frac{d\delta_A}{d\tau} = \left(\frac{\partial \theta}{\partial \eta} \right)_{\delta_B} - \left(\frac{\partial \theta}{\partial \eta} \right)_{\delta_A}. \quad (4)$$

Now a function profile has to be chosen to be used in the dimensionless temperature. In the present paper the Eq. following equation is used:

$$\theta = A \left(\frac{\delta_B - \eta}{\delta_B - \delta_A} \right)^n + B \left(\frac{\delta_B - \eta}{\delta_B - \delta_A} \right) + C. \quad (5)$$

It is important to note that this equation is defined only in the space between δ_A and δ_B , the region left to δ_A , i.e $\eta < \delta_A$, has no physical meaning, and the region right to δ_B ($\eta > \delta_B$) is set equal to zero which means that the temperature is still equal to the initial value T_0 . Substituting Eq. (5) in Eq. (4) one obtains:

$$\frac{d}{d\tau} \left(\left(\frac{A}{n+1} + \frac{B}{2} + C \right) (\delta_B - \delta_A) \right) - C \frac{d\delta_B}{d\tau} + (A+B+C) \frac{d\delta_A}{d\tau} = \frac{An}{(\delta_B - \delta_A)}. \quad (6)$$

This equation is considered, from now on, the main equation for developing of the solutions. It consists of three terms at the left hand side: the first one is the rate of the accumulate energy on the body, the second and third ones are related to the change of energy due to the displacement of the δ_B and δ_A frontiers, respectively. Finally, the right hand side term is the net flow rate of energy between the two frontiers.

To solve the main equation (Eq. 6), the boundary conditions have to be rearranged. Firstly they are non-dimensionalized, using Eq. (2), and then Eq. (5) is used to obtain the profile boundary conditions, useful for the HBIM. This procedure is shown for each boundary condition considered in the present work.

A. Prescribed Temperature (PT) – Dirichlet Condition

The Prescribed Temperature (PT) is the simplest boundary to transform. The value T_{PA} represents the prescribed temperature value at the position Δ_A , while T_{PB} represents the prescribed temperature value at the Δ_B , respectively:

$$X = \Delta_A \rightarrow T = T_{PA}, \quad (7)$$

$$X = \Delta_B \rightarrow T = T_{PB}. \quad (8)$$

Using the transformations indicated at Eq. (2) and substituting Eq. (5), Eqs. (7) and (8) becomes the following equations, which are ready to be applied to the HBIM problem:

$$\eta = \delta_A \rightarrow A + B + C = \theta_{PA}, \quad (9)$$

$$\eta = \delta_B \rightarrow C = \theta_{PB}. \quad (10)$$

B. Prescribed Heat Flux (PH) – Neumann Condition

The Prescribed Heat Flux (PH) boundary conditions are represented by:

$$X = \Delta_A \rightarrow -k \frac{\partial T}{\partial X} = q''_{PA}, \quad (11)$$

$$X = \Delta_B \rightarrow -k \frac{\partial T}{\partial X} = q''_{PB}. \quad (12)$$

Applying the transformations indicated by Eqs. (2) and (5), they take the forms, respectively:

$$\eta = \delta_A \rightarrow \frac{An+B}{\delta_B - \delta_A} = Q_{PA}, \quad (13)$$

$$\eta = \delta_B \rightarrow \frac{B}{\delta_B - \delta_A} = Q_{PB}. \quad (14)$$

In these equations, the q'' parameter represent the heat flux; the positive values indicate that the flux is at the X direction. The Q variable applied in Eqs. 13 and 14, are associated with a relative heat flux, based on the ratio between the incident heat flux and a reference heat flux, defined as $k(T_R - T_O)/L$, as expressed by:

$$Q_{PA} = \frac{q''_{PA} L}{k(T_R - T_O)} \text{ and } Q_{PB} = \frac{q''_{PB} L}{k(T_R - T_O)} \quad (15)$$

C. Semi-Finite (SF) – Half-Space Condition

The Semi-Finite (SF) boundary condition is used at the initial time solutions of the problem, when the point Δ_B has not reached the back face of the solid. So, at Δ_B , the next equation is used as boundary condition (zero prescribed heat flux and prescribed temperature equal to the initial temperature conditions):

$$X = \Delta_B \rightarrow -k \frac{\partial T}{\partial X} = 0 \text{ and } T = T_0 \quad (16)$$

Similarly to the other conditions, these equations are manipulated, using Eqs. (2) and (5) parameters, resulting in:

$$\eta = \delta_b \rightarrow B = 0 \text{ and } C = 0 \quad (17)$$

IV. Heat Balance Integral Method Solutions

In this section, Eq. (6), with the boundaries conditions combinations presented at Fig. 1, is solved analytically using the HBIM.

- **Semi-Finite Solid**

The Semi-Finite Solid condition has already been developed in previous works (Braga et al. (2005)⁶) and the main results are reprinted in Table 2, as they are used as the starting point for the finite solid solutions.

Table 2. Summary of the semi-finite solid solutions

	Prescribed Heat Flux	Prescribed Temperature
Surface Temperature	$A = \frac{Q_{PA} \delta_B}{n}$	$A = \theta_{PA}$
Heat Penetration Depth	$\delta_B = \sqrt{\frac{n(n+1)}{Q_{PA}} \int_0^\tau Q_{PA} d\tau}$	$\delta_B = \sqrt{\frac{2n(n+1)}{\theta_{PA}^2} \int_0^\tau \theta_{PA}^2 d\tau}$
Temperature Profile	$\theta = \sqrt{Q_{PA} \frac{(n+1)}{n} \int_0^\tau Q_{PA} d\tau} \left(1 - \sqrt{\frac{Q_{PA} \eta^2}{n(n+1) \int_0^\tau Q_{PA} d\tau}} \right)^n$	$\theta = \theta_{PA} \left(1 - \sqrt{\frac{\theta_{PA}^2 \eta^2}{2n(n+1) \int_0^\tau \theta_{PA}^2 d\tau}} \right)^n$
Transition Time (τ_m)	$\int_0^{\tau_m} Q_{PA} d\tau = \frac{Q_{PA}}{n(n+1)} (L^2 - \delta_A^2)$	$\int_0^{\tau_m} \theta_{PA}^2 d\tau = \frac{\theta_{PA}^2}{2n(n+1)} (L^2 - \delta_A^2)$

- **Finite Solid**

The Finite Solid condition indicates that the Δ_B point has already reached that back surface of the solid and, consequently the distance between Δ_A and Δ_B , as the U variable are constant values. From this moment on, as already described at the Physical Model section, the opposite boundary conditions have to be considered. So, for many of the boundaries combinations at the finite solid case, the main equation (Eq. 6) can be simplified to the form:

$$\frac{dA}{d\tau} + F_1 A = F_2 \frac{dF_3}{d\tau}, \quad (18)$$

where F_1 and F_2 are time-constant expressions and F_3 is a time-dependent function that varies according to the boundaries combinations. The solution of this equation is:

$$A = \left(\int_{\tau_m}^{\tau} F_2 \frac{dF_3}{d\bar{\tau}} \exp(F_1(\bar{\tau} - \tau_m)) d\bar{\tau} + A_m \right) \exp(-F_1(\tau - \tau_m)), \quad (19)$$

where τ_m is the transition time which indicates the instant that the heat penetration depth reaches the back surface, A_m is the value for the A parameter at the transition time and $\bar{\tau}$, which has the same nature of τ , is a dummy integration variable.

A. Prescribed Temperature/Prescribed Temperature Case

The Prescribed Temperature boundary considered at the back surface, which corresponds to Eq. (10), is used to calculate the C parameter, resulting in:

$$C = \theta_{PB}. \quad (20)$$

Similarly, the Prescribed Temperature boundary at the front surface, Eq. (9), is used to obtain an explicit expression for the B parameter. It is obtained with the substitution of Eq. (20) on Eq. (9), which, after some manipulation, results in:

$$B = \theta_{PA} - \theta_{PB} - A \quad (21)$$

Substituting Eqs. (20) and (21) in Eq. (6), and after rearranging it, one gets the following ordinary differential equation (ODE):

$$\frac{dA}{d\tau} + \frac{2(n+1)n}{(n-1)u^2} A = \frac{(n+1)}{(n-1)} \frac{d}{d\tau} (\theta_{PA} + \theta_{PB}) \quad (22)$$

Comparing Eqs. (22) and (18) the F 's terms can be obtained. After appropriate substitutions on Eq. (19) the following solution is obtained:

$$A = \left(\int_{\tau_m}^{\tau} \frac{(n+1)}{(n-1)} \frac{d}{d\bar{\tau}} (\theta_{PA} + \theta_{PB}) \exp\left(\frac{2(n+1)n(\bar{\tau} - \tau_m)}{(n-1)u^2}\right) d\bar{\tau} + A_m \right) \exp\left(-\frac{2(n+1)n(\tau - \tau_m)}{(n-1)u^2}\right). \quad (23)$$

Now, the dimensionless temperature profile, given by Eq. (5), can be obtained, after the substitution of Eqs. (20), (21) and (23), resulting in:

$$\theta = \left(\int_{\tau_m}^{\tau} \frac{(n+1)}{(n-1)} \frac{d}{d\bar{\tau}} (\theta_{PA} + \theta_{PB}) \exp\left(\frac{2(n+1)n(\bar{\tau} - \tau_m)}{(n-1)u^2}\right) d\bar{\tau} + A_m \right) \exp\left(-\frac{2(n+1)n(\tau - \tau_m)}{(n-1)u^2}\right) \left(\left(\frac{\delta_B - \eta}{u}\right)^n - \left(\frac{\delta_B - \eta}{u}\right) \right) + (\theta_{PA} - \theta_{PB}) \left(\frac{\delta_B - \eta}{u}\right) + \theta_{PB} \quad (24)$$

B. Prescribed Temperature/ Prescribed Heat Flux Case

The Prescribed Heat Flux boundary considered at the back surface, which correspond to Eq. (14) is used to calculate the Eq. (5) B parameter, resulting in:

$$B = Q_{PB} u \quad (25)$$

For this case, the Prescribed Temperature boundary at the front surface, Eq. (09), is used to obtain an explicit expression for the C parameter. Substituting Eq. (25) on Eq. (09) and after some manipulation, one finally gets:

$$C = \theta_{PA} - Q_{PB} u - A \quad (26)$$

Substituting Eqs. (25) and (26) at Eq. (6) and after rearranging the resulting expression, one gets the following ODE:

$$\frac{dA}{d\tau} + \frac{n+1}{u^2} A = \frac{n+1}{n} \frac{d}{d\tau} \left(\theta_{PA} - \frac{Q_{PB} u}{2} \right) \quad (27)$$

Comparing Eqs. (27) and (18), the F terms can be obtained. Making the appropriate substitutions on Eq. (19) the solution bellow is obtained:

$$A = \left(\int_{\tau_m}^{\tau} \frac{n+1}{n} \frac{d}{d\bar{\tau}} \left(\theta_{PA} - \frac{Q_{PB} u}{2} \right) \exp\left(\frac{(n+1)(\bar{\tau} - \tau_m)}{u^2}\right) d\bar{\tau} + A_m \right) \exp\left(-\frac{(n+1)(\tau - \tau_m)}{u^2}\right) \quad (28)$$

The dimensionless temperature profile can be obtained after the substitution of Eqs. (25), (26) and (28) in Eq. (5), resulting in:

$$\theta = \left(\int_{\tau_m}^{\tau} \frac{n+1}{n} \frac{d}{d\bar{\tau}} \left(\theta_{PA} - \frac{Q_{PB} u}{2} \right) \exp\left(\frac{(n+1)(\bar{\tau} - \tau_m)}{u^2}\right) d\bar{\tau} + A_m \right) \exp\left(-\frac{(n+1)(\tau - \tau_m)}{u^2}\right) \left(\left(\frac{\delta_B - \eta}{u}\right)^n - 1 \right) - Q_{PB} (\delta_B - \eta - u) + \theta_{PA} \quad (29)$$

C. Prescribed Heat Flux/ Prescribed Temperature Case

The Prescribed Temperature boundary considered at the back surface, which corresponds to Eq. (10) is used to calculate the C parameter, given by:

$$C = \theta_{PB} \quad (30)$$

The Prescribed Heat Flux boundary at the front surface, Eq. (13), is used to get an explicit expression for the B parameter. It is obtained with the substitution of Eq. (30) on Eq. (13). After some manipulation, one gets:

$$B = Q_{PA} u - A n \quad (31)$$

Substituting Eqs. (30) and (31) in Eq. (6), one gets the following ODE, after some manipulation:

$$\frac{dA}{d\tau} + \frac{2n(n+1)}{(n(n+1)-2)u^2} A = \frac{2(n+1)}{n(n+1)-2} \frac{d}{d\tau} \left(\frac{Q_{PA} u}{2} + \theta_{PB} \right) \quad (32)$$

Comparing Eqs. (32) and (18), the F terms can be obtained. Making the appropriate substitutions on Eq. (19), the solution below is obtained:

$$A = \left(\int_{\tau_m}^{\tau} \frac{2(n+1)}{n(n+1)-2} \frac{d}{d\bar{\tau}} \left(\frac{Q_{PA} u}{2} + \theta_{PB} \right) \exp \left(\frac{2n(n+1)(\bar{\tau}-\tau_m)}{(n(n+1)-2)u^2} \right) d\bar{\tau} + A_m \right) \exp \left(-\frac{2n(n+1)(\tau-\tau_m)}{(n(n+1)-2)u^2} \right) \quad (33)$$

After the substitution of Eqs. (30), (31) and (33) in the dimensionless temperature profile, Eq. (5), the following equation can be found:

$$\theta = \left(\int_{\tau_m}^{\tau} \frac{2(n+1)}{n(n+1)-2} \frac{d}{d\bar{\tau}} \left(\frac{Q_{PA} u}{2} + \theta_{PB} \right) \exp \left(\frac{2n(n+1)(\bar{\tau}-\tau_m)}{(n(n+1)-2)u^2} \right) d\bar{\tau} + A_m \right) \exp \left(-\frac{2n(n+1)(\tau-\tau_m)}{(n(n+1)-2)u^2} \right) \left(\left(\frac{\delta_B - \eta}{u} \right)^n - n \left(\frac{\delta_B - \eta}{u} \right) \right) + Q_{PA} (\delta_B - \eta) + \theta_{PB} \quad (34)$$

D. Prescribed Heat Flux/ Prescribed Heat Flux Case

The Prescribed Heat Flux boundary considered at the back surface, given by Eq. (14), is used to calculate the B parameter, resulting in:

$$B = Q_{PB} u. \quad (35)$$

The Prescribed Heat Flux boundary at the front surface, Eq. (13), is used to get an explicit expression for the A parameter. It is obtained with the substitution of Eq. (35) on Eq. (13), which, after some manipulation, results in:

$$A = (Q_{PA} - Q_{PB}) \frac{u}{n} \quad (36)$$

Substituting Eqs. (35) and (36) in Eq. (6), after some rearrangement, one gets the following ODE

$$\frac{dC}{d\tau} = \frac{(Q_{PA} - Q_{PB})}{u} - \frac{d}{d\tau} \left(\frac{(Q_{PA} - Q_{PB})u}{n(n+1)} + \frac{Q_{PB} u}{2} \right), \quad (37)$$

which is easily solved obtaining

$$C = \int_{\tau_m}^{\tau} \frac{(Q_{PA} - Q_{PB})}{u} d\bar{\tau} - \left(\frac{(Q_{PA} - Q_{PB})u}{n(n+1)} + \frac{Q_{PB} u}{2} \right)_{\bar{\tau}=\tau} + \left(\frac{(Q_{PA} - Q_{PB})u}{n(n+1)} + \frac{Q_{PB} u}{2} \right)_{\bar{\tau}=\tau_m}. \quad (38)$$

The dimensionless temperature profile is given by Eq. (5), after the substitution of Eqs. (35), (36) and (38), resulting in:

$$\theta = (Q_{PA} - Q_{PB}) \frac{u}{n} \left(\frac{\delta_B - \eta}{u} \right)^n + Q_{PB} (\delta_B - \eta) + \int_{\tau_m}^{\tau} \frac{(Q_{PA} - Q_{PB})}{u} d\bar{\tau} - \left(\frac{(Q_{PA} - Q_{PB})u}{n(n+1)} + \frac{Q_{PB}u}{2} \right)_{\bar{\tau}=\tau} + \left(\frac{(Q_{PA} - Q_{PB})u}{n(n+1)} + \frac{Q_{PB}u}{2} \right)_{\bar{\tau}=\tau_m} \quad (39)$$

V. Classical Solution

In this section, literature solutions, which will be compared with the HBIM solutions in the next section, are shown. The classical solutions are usually obtained using the Laplace Transform Technique (LTT) or using the Method of Separation of Variables (MSV). These techniques are available in many classical conduction heat transfer books, such as Carslaw & Jaeger (1959)⁸ and Arpaci (1966)⁹, among others. From these solutions, it is possible to obtain the Green's Functions (GF), which actually represents building blocks for more complex solutions, as shown in Beck et al. (1992)¹⁰. In the present paper, the GF method solutions are selected for comparison with the HBIM's solutions. These solutions are presented as shown by Beck et al. (1992)¹⁰ and the important equations are presented below.

- Prescribed Temperature/Prescribed Temperature:

$$\theta(\eta, \tau) = \int_0^{\tau} \theta_{PA} \sum_{m=1}^{\infty} 2m\pi \exp(-m^2 \pi^2 (\tau - \bar{\tau})) \sin(m\pi\eta) d\bar{\tau} - \int_0^{\tau} \theta_{PB} \sum_{m=1}^{\infty} 2(-1)^m m\pi \exp(-m^2 \pi^2 (\tau - \bar{\tau})) \sin(m\pi\eta) d\bar{\tau} \quad (40)$$

- Prescribed Temperature/Prescribed Heat Flux:

$$\theta(\eta, \tau) = \int_0^{\tau} \theta_{PA} \sum_{m=1}^{\infty} (2m-1)\pi \exp\left(-\frac{(2m-1)^2}{4} \pi^2 (\tau - \bar{\tau})\right) \sin\left(\frac{(2m-1)}{2} \pi\eta\right) d\bar{\tau} - \int_0^{\tau} Q_{PB} \sum_{m=1}^{\infty} 2(-1)^m \exp\left(-\frac{(2m-1)^2}{4} \pi^2 (\tau - \bar{\tau})\right) \sin\left(\frac{(2m-1)}{2} \pi\eta\right) d\bar{\tau} \quad (41)$$

- Prescribed Heat Flux/Prescribed Temperature:

$$\theta(\eta, \tau) = \int_0^{\tau} Q_{PA} \sum_{m=1}^{\infty} 2 \exp\left(-\frac{(2m-1)^2}{4} (\tau - \bar{\tau})\right) \cos\left(\frac{(2m-1)}{2} \pi\eta\right) d\bar{\tau} + \int_0^{\tau} \theta_{PB} \sum_{m=1}^{\infty} (2m-1)(-1)^{m+1} \pi \exp\left(-\frac{(2m-1)^2}{4} (\tau - \bar{\tau})\right) \cos\left(\frac{(2m-1)}{2} \pi\eta\right) d\bar{\tau} \quad (42)$$

- Prescribed Heat Flux/Prescribed Heat Flux:

$$\theta(\eta, \tau) = \int_0^{\tau} Q_{PA} + \sum_{m=1}^{\infty} 2Q_{PA} \exp(-m^2 \pi^2 (\tau - \bar{\tau})) \cos(m\pi\eta) d\bar{\tau} + \int_0^{\tau} Q_{PB} + \sum_{m=1}^{\infty} 2(-1)^m Q_{PB} \exp(-m^2 \pi^2 (\tau - \bar{\tau})) \cos(m\pi\eta) d\bar{\tau} \quad (43)$$

VI. Comparison between the solutions

In order to make a comparison between the HBIM and the GF classical solutions, four simple problems are considered. Each one of the problems is related with one of the different boundaries combinations. The prescribed heat fluxes, as well as the prescribed temperatures at the boundaries are considered time-constant, although the previous development does not make use of this simplification.

I. Problem 1: $\theta_{PA} = 1$ and $\theta_{PB} = 0$.

The complete HBIM solution for this problem is

$$\theta(\eta, \tau) = \begin{cases} \left(1 - \sqrt{\frac{\eta^2}{2n(n+1)\tau}}\right)^n, & \eta < \sqrt{2n(n+1)\tau} \\ 0, & \eta > \sqrt{2n(n+1)\tau} \end{cases}, \tau < (2n(n+1))^{-1} \quad (44)$$

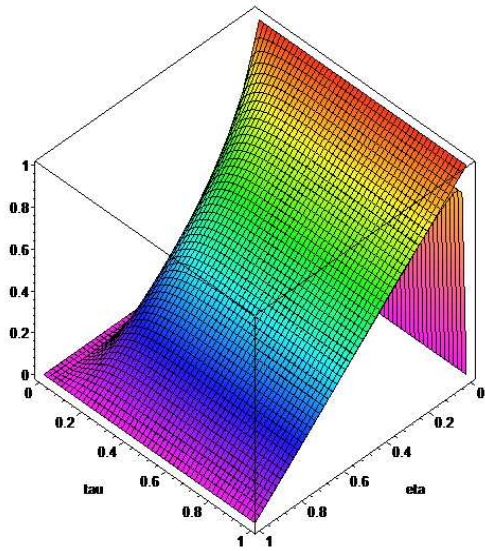
$$\exp\left(\frac{1}{(n-1)} - \frac{2(n+1)n\tau}{(n-1)}\right) \left((1-\eta)^n - (1-\eta)\right) + (1-\eta), \quad \tau > (2n(n+1))^{-1}$$

and the GF solution is

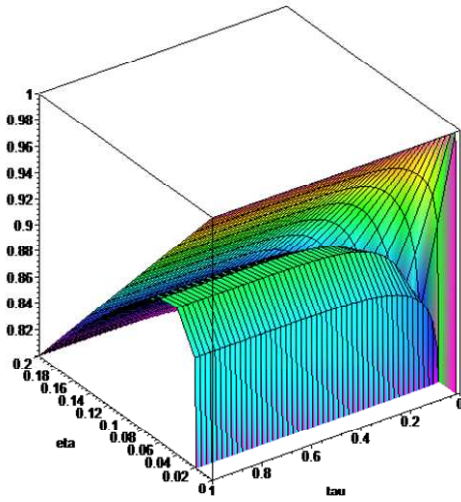
$$\theta(\eta, \tau) = \sum_{m=1}^{\infty} \frac{2 \sin(m\pi\eta)}{m\pi} (1 - \exp(-m^2 \pi^2 \tau)) \quad (45)$$

Usually the best n value for the HBIM solution can be obtained comparing the heat flux of both solutions at the same point, usually at the front surface. But this procedure cannot be applied using the GF solution due the sin characteristic of the solution, which vanishes at the boundary and the heat flux result at the same point would be a fake. In this case, a good option is to use the same n value obtained for the prescribed temperature boundary condition at the half-space domain, which is $2/(\pi-2) \sim 1.75$ (presented at Braga et al. (2005)⁶).

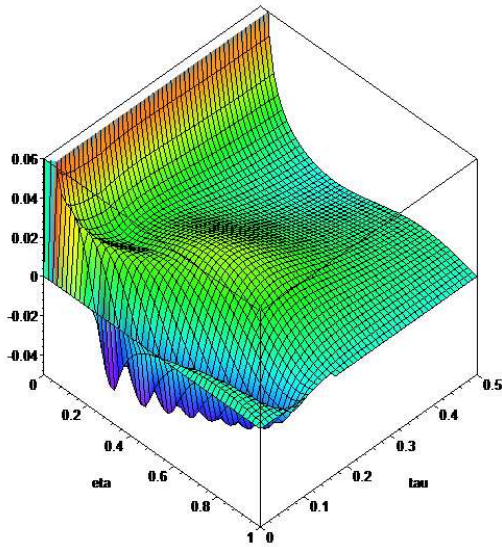
Figure 2 presents three graphics: the first one (a) shows two surfaces, one for the non-dimensional temperature of the HBIM solution and other for the GF solution, as a function of the non dimensional distance η and of the non dimensional time τ . One can see from this figure that it is very difficult to detect a difference between these surfaces, with exception to the position $\eta=0$. The second figure (b) presents a detail of the difference between the solutions near the $\eta=0$ position, and in the third graphic (c) the difference between those solutions is shown, both as functions of η and τ . The largest difference occurs at the boundary and vanishes as η increase. The second difference source is close the transition time period, τ_m , and this difference can be explained due the semi-finite characteristic of the solution used at the first dominium region (se Eq. 44, $\tau < (2n(n+1))^{-1}$) of the HBIM. It is important to note that the difference is less than 6% for the major part of the domain.



(a) HBIM and GF Solutions

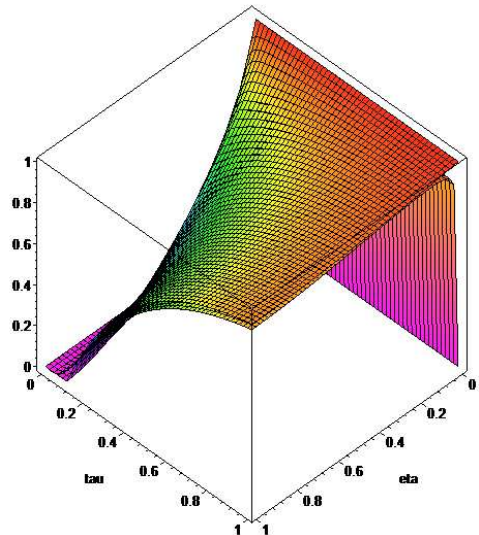


(b) Detail of the solutions near $\eta = 0$.

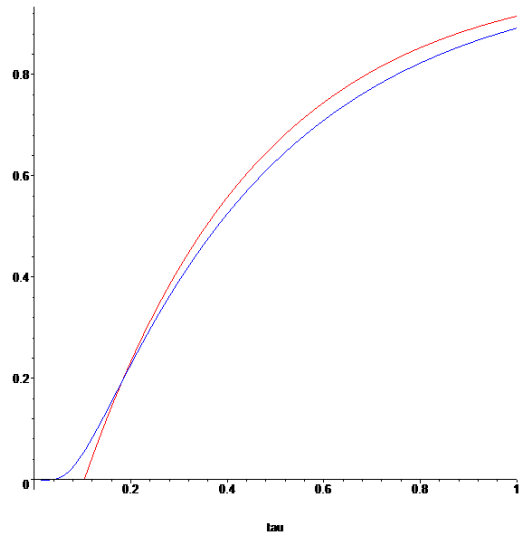


(c) Difference of the solutions (HBIM - GF)

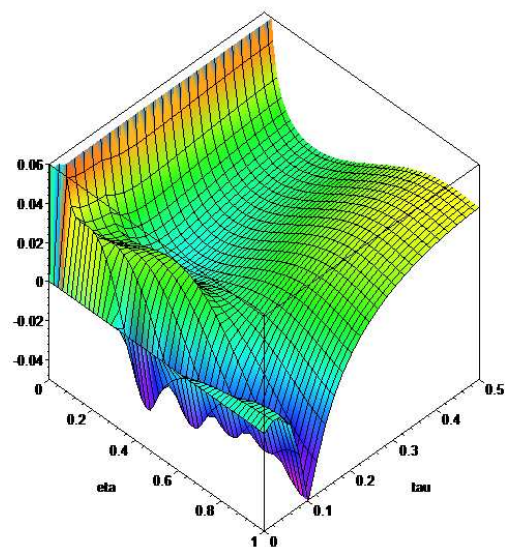
Figure 2. Comparison of the solutions at problem 1 situation



(a) HBIM and GF Solutions



(b) Solutions at $\eta = 0$ (blue: GF; red: HBIM)



(c) Difference of the solutions (HBIM - GF)

Figure 3. Comparison of the solutions at problem 2 situation

II. Problem 2: $\theta_{PA} = 1$ and $Q_{PB} = 0$.

The complete HBIM solution equation for this problem is:

$$\theta(\eta, \tau) = \begin{cases} \left(1 - \sqrt{\frac{\eta^2}{2n(n+1)\tau}}\right)^n, & \eta < \sqrt{2n(n+1)\tau}, \tau < (2n(n+1))^{-1} \\ 0, & \eta > \sqrt{2n(n+1)\tau} \\ \exp\left(\frac{1}{2n} - (n+1)\tau\right) \left((1-\eta)^n - 1\right) + 1, & \tau > (2n(n+1))^{-1} \end{cases} \quad (46)$$

and the GF is:

$$\theta(\eta, \tau) = \sum_{m=1}^{\infty} \frac{4 \sin\left(\frac{(2m-1)\pi\eta}{2}\right)}{(2m-1)\pi} \left(1 - \exp\left(-\frac{(2m-1)^2 \pi^2 \tau}{4}\right)\right) \quad (47)$$

Similarly to the problem 1 solution, which deals with prescribed temperature at the front surface, the investigation of the n value cannot be performed at the boundary position and the same value used for problem 1 is employed.

Figure 3 presents three graphics. The first one (a) shows the plotting of two surfaces corresponding to the non-dimensional temperature of the HBIM and GF solutions, as a function of the parameter η and τ . The largest differences between these solutions are observed in the same position as in problem 1, at the front surface and at the opposite boundary, due the transition time in which starts the influence of the boundary condition in the solution. The second graph (b) presents a two dimensional plot of the non dimensional temperature as a function of the non dimensional time for both solutions, at the $\eta=1$ position: one can observe that the GF solution (blue line) is early influenced by the boundary condition, when compared with the HBIM solution (red line), as explained before; and at the third graphic (c) it is presented the absolute difference between those two solutions, in a surface similar to the graph (a). The largest difference occurs at the boundary and vanishes as η increase. The second difference source is close the transition time period, τ_m , and this difference can be explained due the semi-finite characteristic of the solution used at the first dominium region (se Eq. 46, $\tau < (2n(n+1))^{-1}$) of the HBIM. It is important to note that the difference is less than 6% for the major part of the domain.

III. Problem 3: $Q_{PA} = 1$ and $\theta_{PB} = 0$.

The complete HBIM solution for problem 3 is:

$$\theta(\eta, \tau) = \begin{cases} \sqrt{\frac{(n+1)}{n}} \tau \left(1 - \sqrt{\frac{\eta^2}{n(n+1)\tau}}\right)^n, & \eta < \sqrt{n(n+1)\tau}, \tau < (n(n+1))^{-1} \\ 0, & \eta > \sqrt{n(n+1)\tau} \\ \frac{1}{n} \exp\left(\frac{2-2n(n+1)\tau}{(n(n+1)-2)}\right) \left((1-\eta)^n - n(1-\eta)\right) + (1-\eta), & \tau > (n(n+1))^{-1} \end{cases}, \quad (48)$$

and the GF solution is:

$$\theta(\eta, \tau) = \sum_{m=1}^{\infty} \frac{8 \cos\left(\frac{(2m-1)\pi\eta}{2}\right)}{(2m-1)^2 \pi^2} \left(1 - \exp\left(-\frac{(2m-1)^2 \pi^2 \tau}{4}\right)\right) \quad (49)$$

From latter work (Braga et al. (2005)⁶), a value of $n = \pi/(4-\pi) \sim 3.67$ was suggested based on a comparison with the half-space classic solution. In the present case the same value is considered.

Figure 4 presents three graphics: the first one (a) shows the plot of two non-dimensional temperature surfaces for the HBIM and GF solutions as a function of η and τ . It can be shown that the largest difference occurs at the front surface, $\eta = 0$. This difference can be better observed by the second plot (b), which relates the non dimensional temperature with the non-dimensional time of the two analytical solutions at the $\eta = 0$ position. The GF solution is represented by the blue line and the HBIM solution by the red line. With this plot, it can be seen that the difference occurs only at the second dominium region (se Eq. 48, $\tau > (n(n+1))^{-1}$) of the HBIM solution and it occurs due the n selected value, another choice of this value leads to a better agreement at this part of the solution but will increase the difference at the first dominium region.

The third graphic (c) shows the difference between the two solutions, through a surface similar to the plot (a) graph. The largest difference between solutions is observed at the boundary $\eta = 0$ and this difference vanishes as η increases. The second largest difference source is found in the region close to the transition time, τ_m , due the change at the dominium region of the HBIM solution. It is important to notice that the difference is less than 1% in the largest region of the domain.

IV. Problem 4: $Q_{PA} = 1$ and $Q_{PB} = 0$.

The complete HBIM solution for this problem is given by the equation:

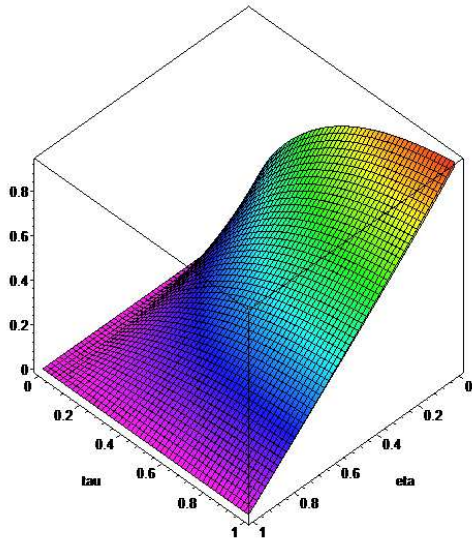
$$\theta(\eta, \tau) = \begin{cases} \left\{ \sqrt{\frac{(n+1)}{n}} \tau \left(1 - \sqrt{\frac{\eta^2}{n(n+1)\tau}}\right)^n, & \eta < \sqrt{n(n+1)\tau} \\ 0, & \eta > \sqrt{n(n+1)\tau} \right. & , \tau < (n(n+1))^{-1} \\ \left. \frac{(1-\eta)^n}{n} + \tau - \frac{1}{n(n+1)}, & & , \tau > (n(n+1))^{-1} \right. \end{cases} \quad (50)$$

while the GF solution is:

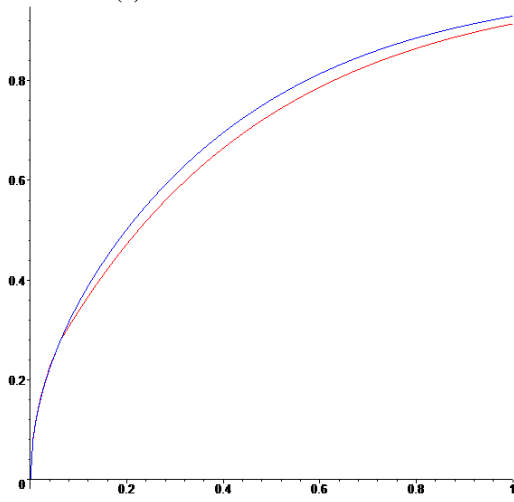
$$\theta(\eta, \tau) = \tau + \sum_{m=1}^{\infty} \frac{2 \cos(m\pi\eta)}{m^2 \pi^2} (1 - \exp(-m^2 \pi^2 \tau)) \quad (51)$$

In this problem the same n value of the problem 3 is applied because the starting point of the solution is the same (half-space with prescribed heat flux).

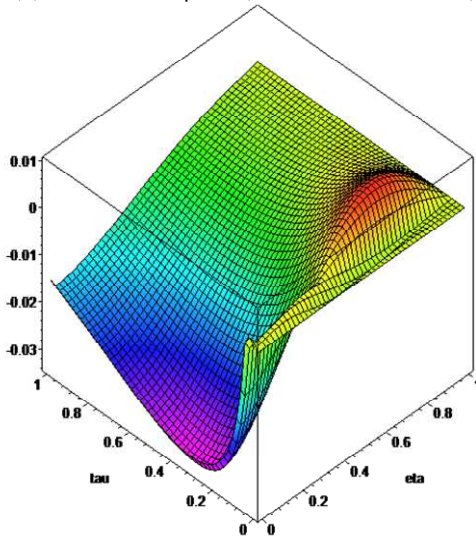
Figure 5 presents three graphics: the first one (a) shows the surface plot of the non-dimensional temperature of the HBIM and GF solutions as a function of η and τ . A difference between the solutions is observed and it is due to the adopted n value; a different n value would present other differences. It is important to note that the good agreement between the solutions observed at the the first dominium region (se Eq. 50, $\tau < (n(n+1))^{-1}$) of the HBIM solution does not persists for the second region. The difference between solution increases with the increasing non dimensional time, as it can be observed through the second plot (b), that presents a detailed plot of the non dimensional temperature solutions as a function of the non-dimensional space, for the non-dimensional time $\tau=1$. The GF solution is represented by the blue line and the HBIM solution by the red one. The third graphic (c) is a surface plot of the difference between the two solutions as a function of η and τ . The largest differences happen at the boundaries and at this position they increase as time increases. It is important to note that even with this discrepancy, the difference is less than 10% in the larger region of the domain.



(a) HBIM and GF Solutions

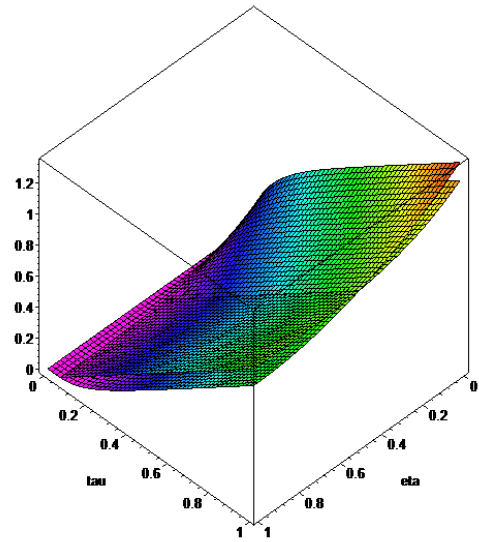


(b) Solutions at $\eta = 0$ (blue: GF; red: HBIM)

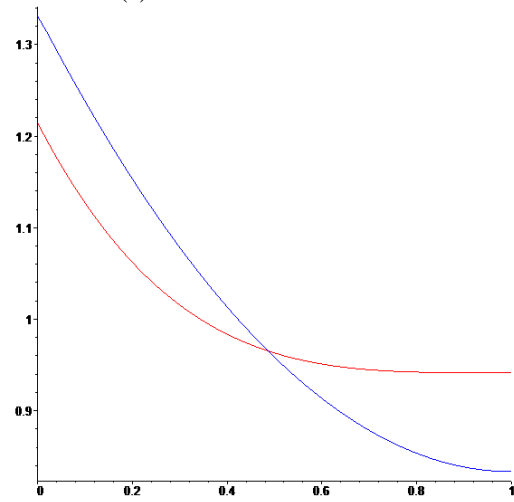


(c) Difference of the solutions (HBIM - GF)

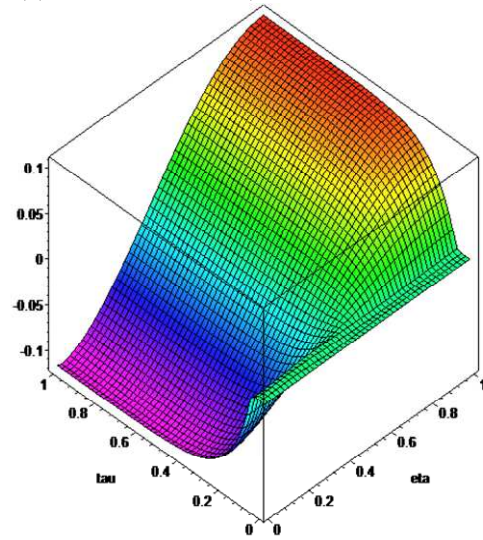
Figure 4. Comparison of the solutions at problem 3 situation



(a) HBIM and GF Solutions



(b) Solutions at $\tau = 1$ (Blue: GF, Red: HBIM)



(c) Difference of the solutions (HBIM - GF)

Figure 5. Comparison of the solutions at problem 4 situation

VII. Conclusion

In this paper the Heat Balance Integral Method was used to solve the heat conduction problem inside a one dimensional finite solid body, subjected to four different combinations of the boundaries conditions. As part of the method, an n degree function was selected as representative of the temperature distribution of the material. The value of the n was selected as the same for the parts of the solution, where half-space and finite solid are considered, as previously determinate at Braga et al. (2005)⁶. It is important to note that the best n value is not a closed subject and hard work still is necessary for the development of the method.

Four different cases were solved and their results compared with a literature solutions presenting a very good agreement. The traditional literature methods are exact while the HBIM are approximate methods. The HBIM advantages dealing with linear problems are: 1) easy solution: the HBIM involves the solution of only one ODE while the exact methods are based on the solution of PDEs; 2) fast calculus: the HBIM solution are faster to be obtained than the exact one because it does not depend on any eigenvalue, eigenfunction or series arithmetic; 3) the HBIM helps to get a better understanding of the cause-effect between the non dimensional parameters and the obtained solution physics.

References

- ¹ Braga, W. F., Mantelli, M.B.H., "Electrical Analogy Modeling for One-Dimensional Ablation Problem", 8th AIAA/ASME Joint Thermophysics and Heat Transfer Conference, AIAA, Washington, DC, 2002.
- ² Braga, W.F., Mantelli, M.B.H., Azevedo, J.L.F., "Approximated Analytical Solution for One-Dimensional Ablation Problem with Time-Variable Heat Flux", 36th AIAA Thermophysics Conference, AIAA, Washington, DC, 2003.
- ³ Braga, W.F., Mantelli, M.B.H., Azevedo, J.L.F., "Approximated Analytical Solution for One-Dimensional Finite Ablation Problem with Constant Time Heat Flux", 37th AIAA Thermophysics Conference, AIAA, Washington, DC, 2004.
- ⁴ Goodman, T.R., "Application of Integral Methods to Transient Nonlinear Heat Transfer", Advances in Heat Transfer, Vol. 1, Academic Press, New York, 1964, pp. 51 – 122.
- ⁵ Goodman, T.R., "This Week's Citation Classic – The heat-balance integral and its application to problems involving a change of phase", Current Contents ET&AS, Number 23, June 06, 1983, URL.: <http://garfield.library.upenn.edu/classics1983/A1983QR38700001.pdf>. [cited 01 november 2008].
- ⁶ Braga, W.F., Mantelli, M.B.H., Azevedo, J.L.F., "A New Approach for the Heat Balance Integral Method Applied to Heat Conduction Problems", 43rd AIAA Aerospace Sciences Meeting and Exhibit, AIAA, Washington, DC, 2005.
- ⁷ Braga, W.F., Mantelli, M.B.H., Azevedo, J.L.F., "Analytical Solution for One-Dimensional Semi-Infinite Heat Transfer Problem with Convection Boundary Condition", 38th AIAA Thermophysics Conference, AIAA, Washington, DC, 2005.
- ⁸ Carslaw, H.S., Jaeger, J.C., "Conduction of Heat in Solids", 2nd ed., Oxford University Press, London, 1959.
- ⁹ Arpaci, V. S., "Conduction Heat Transfer", Addison-Wesley Publishing Company, Menlo Park, California, 1966.
- ¹⁰ Beck, J. V., Cole, K. D., Haji-Sheikh, A., Litkouhi, B., "Heat Conduction Using Green's Function", Hemisphere Publishing Corporation, Washington, DC, 1992.